

ARTICLE OPEN



Resting-state brain activation patterns and network topology distinguish human sign and goal trackers

Martino Schettino^{1,2,8}, Marika Mauti^{1,3,8}, Chiara Parrillo⁴, Ilenia Ceccarelli⁵, Federico Giove^{6,7}, Antonio Napolitano⁴, Cristina Ottaviani^{1,7}, Marialuisa Martelli¹ and Cristina Orsini^{1,7}✉

© The Author(s) 2024

The “Sign-tracker/Goal-tracker” (ST/GT) is an animal model of individual differences in learning and motivational processes attributable to distinctive conditioned responses to environmental cues. While GT rats value the reward-predictive cue as a mere predictor, ST rats attribute it with incentive salience, engaging in aberrant reward-seeking behaviors that mirror those of impulse control disorders. Given its potential clinical value, the present study aimed to map such model onto humans and investigated resting state functional magnetic resonance imaging correlates of individuals categorized as more disposed to sign-tracking or goal-tracking behavior. To do so, eye-tracking was used during a translationally informed Pavlovian paradigm to classify humans as STs ($n = 36$) GTs ($n = 35$) or as Intermediates ($n = 33$), depending on their eye-gaze towards the reward-predictive cue or the reward location. Using connectivity and network-based approach, measures of resting state functional connectivity and centrality (role of a node as a hub) replicated preclinical findings, suggesting a major involvement of subcortical areas in STs, and dominant cortical involvement in GTs. Overall, the study strengthens the translational value of the ST/GT model, with important implications for the early identification of vulnerable phenotypes for psychopathological conditions such as substance use disorder.

Translational Psychiatry (2024)14:446; <https://doi.org/10.1038/s41398-024-03162-w>

INTRODUCTION

In preclinical literature, sign-tracking behavior is regarded as an expression of attraction to reward-associated stimuli, due to their acquired motivational significance through conditioning. Notably, such attraction only emerges in individuals who attribute incentive salience to the reward-predictive cue, as described in the rodent model of phenotypical variation known as “Sign-tracker/Goal-tracker” (ST/GT) [1]. In an outbred population of rats trained in the Pavlovian Conditioned Approach paradigm (PCA) – where the appearance of a lever (cue) precedes the delivery of a sweet food reward – three behavioral phenotypes emerged after repeated cue-reward presentations: (i) STs readily approaching the cue during its presentation; (ii) GTs approaching the empty location where the reward would be delivered in the future, and (iii) Intermediates (Int) alternating between approaching the cue and the empty location [1]. Only for STs, does the discrete cue acquire motivational properties of its own and become a conditioned reinforcer, whereas for GTs, it is the contextual cue that exerts control over behavior [2]. Thus, the development of a sign-tracking versus goal-tracking conditioned response depends on distinctive associative processes in the use of reward-predictive information. The behavior of STs aligns with a “model free” and dopamine-dependent assessment of the reward-predictive cue (also known as reward prediction error learning), while the behavior of GTs indicates a representational process and is

consistent with a “model based” assessment of the reward-predictive cue [3, 4]. These Pavlovian valuation systems compete for control of behavior but are not entirely independent, as they both converge in the ventral striatum [5]. Dopaminergic signaling within the ventral striatum, specifically within the core of the Nucleus Accumbens (NAc), is critical for the development and expression of ST behavior [3, 6, 7], aligning with dopamine’s role in attributing incentive salience [8]. However, while a bottom-up input from subcortical areas predominates in the ST phenotype, a top-down cortical input controls behavior in the GT phenotype. Both types of input modulate the ventral striatum via the paraventricular nucleus of the thalamus (PVT), which acts as a crucial mediator of both bottom-up and top-down control of cue-motivated behavior [9, 10].

Although the propensity to attribute salience to Pavlovian reward-predictive cues is not inherently pathological, highly attractive cues may motivate maladaptive behavioral patterns. Preclinical evidence suggests that the ST phenotype may be a behavioral marker of vulnerability to psychopathology. Indeed, sign-tracking is considered an endophenotype for addictive behavior in general [11–13] and for substance use disorder in particular, as drug-related cues trigger drug craving and relapse in humans [14, 15]. In fact, cocaine-related cues acquire considerable motivational power [16] and reinforce greater reinstatement of drug seeking behavior in ST rats only [17, 18]. Compared to GT

¹Department of Psychology, Sapienza University of Rome, Rome, Italy. ²IRCCS Istituto delle Scienze Neurologiche di Bologna, Bologna, Italy. ³Area of Neuroscience, SISSA, Trieste, Italy. ⁴Bambino Gesù Children’s Hospital, Rome, Italy. ⁵Department of Medical and Surgical Sciences, University of Bologna, Bologna, Italy. ⁶Museo storico della fisica e Centro studi e Ricerche Enrico Fermi, Rome, Italy. ⁷IRCCS Santa Lucia Foundation, Rome, Italy. ⁸These authors contributed equally: Martino Schettino, Marika Mauti.

✉email: cristina.ottaviani@uniroma1.it

Received: 2 October 2023 Revised: 8 October 2024 Accepted: 11 October 2024

Published online: 22 October 2024

rats, ST rats acquire cocaine self-administration more quickly [19], choose cocaine over food more often [20], show higher motivation for cocaine, and persist in drug-seeking despite negative consequences [21]. Moreover, the ST phenotype is associated with common features of addictive disorders, such as higher impulsivity [22–27] and increased attentional bias for reward-predictive cues [28–31]. Overall, sign-tracking appears to be an addiction-prone endophenotype characterized by unrestrained emotional and motivational responses to reward/drug-predictive cues, co-segregating with impulsivity and poor attentional control.

In humans, individual differences in sensitivity to conditioned stimuli have been primarily investigated in individuals with drug addiction, who exhibit higher “cue-reactivity” (i.e., automatic attraction, capture of attention, attentional bias) for drug-predictive cues and cue-induced craving [30, 31]. However, it should be noted that reward-predictive cues may also trigger automatic attraction and craving in healthy individuals [32, 33], suggesting that the propensity to assign incentive salience to reward-predictive cues is evident prior to drug-experience and might have predictive value for addiction [34, 35].

Recent attempts to find ST/GT phenotypical variation in healthy individuals have yielded preliminary evidence that, similar to rats, human sign-tracking behavior may be associated with (i) impulsivity [36–38], (ii) model-free learning in the ventral striatum [39], and (iii) subcortical activation during reward processing [40]. The ST/GT categorization has been replicated in humans by assessing the eye-gaze on the sign versus the goal location on a computer screen [37, 39, 41], as well as by physical interaction (i.e., touch) with the sign versus the goal location [38, 40]. Overall, results suggest that both eye-tracking and behavioral measures can capture the psychological processes underlying ST/GT phenotypical variations in humans.

Among the reviewed translational attempts, two studies also performed functional magnetic resonance imaging (fMRI) during a Pavlovian conditioning task [39] and a Monetary Incentive Delay task [40] to test whether ST/GT phenotypes were characterized by distinctive patterns of task-related brain responses. The first study [39] described a model-free reward prediction error signal in the ventral striatum in STs but not in GTs, while the second [40] reported an association of amygdala activation during reward anticipation with attentional and inhibitory control deficits in STs.

To the best of our knowledge, no studies have investigated whether the ST/GT phenotype could be predicted by different patterns of resting state functional connectivity and network topology, which refers to the temporal synchronization of spontaneous neuronal activity in anatomically separated regions and functional brain networks. This represents an important unmet need, considering that the phenotypical expression of sign- and goal-tracking may be linked to subtle but relevant differences in the functional architecture of cortico-striatal-thalamic circuits, as suggested by studies in rodents [10, 28, 42]. Compared to existing task-related fMRI attempts, resting state fMRI has the potential to predict both adaptive and maladaptive behaviors [43] and seems to be the most suitable approach to detect trait (i.e., putatively stable) differences, such as sign- and goal-tracking behaviors. Here, a new translationally-relevant PCA task based on eye-gaze was developed to assess the ST/GT phenotypical variation in a population of psychiatrically healthy participants. Neural correlates of sign- and goal-tracking behaviors were derived from brain topology and functional connectivity during resting state fMRI.

MATERIALS AND METHODS

Sample

An a priori power analysis using G*Power software was performed based on existing studies of sign-tracking and goal-tracking in humans [37, 40]. The analysis indicated the need to enroll a sample of 56 participants to

detect a large effect with 80% power. Considering that we did not screen for contraindications for fMRI studies, and given that commonly about 50% of young adults do not meet such criteria, we opted for recruiting 112 participants.

Eighty females and thirty-two males (mean age 21.22 ± 3.09 years) were enrolled by word of mouth and flyers after providing written informed consent to a protocol approved by the Institutional Review Board of the Department of Psychology (Prot. N. 547/2021) and by the Research Ethical Committee of IRCSS Santa Lucia Foundation (CE/PROG.896). Participants were excluded from the study if they exhibited: (a) a history or presence of serious medical conditions (pacemaker, cardiac arrhythmia, hypertension, diabetes, endocrine or metabolic disorders); (b) psychiatric disorders (including drug addiction); (c) neurological disorders including traumatic brain injury, history of childhood neurological disorders; (d) use of specific medications (i.e., SSRI/SNRI, sedative-hypnotic or psychotropic medications, antiepileptic drugs) within 1 week prior screening; (e) obesity (body mass index $> 30 \text{ kg/m}^2$); (f) pregnancy or breastfeeding. After the exclusion of 3 participants, the final sample that participated in the behavioral phase of the study comprised 109 participants (77 females; 20 ± 3.11 years). The sample was not diverse in terms of ethnicity (100% white individuals).

Among them, a subsample of 44 individuals (24 females; 21.21 ± 2.65 years) met the additional requirements for fMRI studies (e.g., absence of metallic implants) and completed also the second phase. All participants were compensated for their time after completing the behavioral task (20 euros) and the fMRI session (an additional 30 euros).

Procedure

After reading and signing the informed consent, participants were asked to complete a series of online questionnaires via Qualtrics, assessing socio-demographic and medical information (e.g., sex, age, education level, medical or psychiatric diagnosis, substance use). If inclusion criteria were met, participants were subsequently evaluated for the dispositional psychological characteristics shown to co-segregate with ST/GT (e.g., impulsiveness, obsessive-compulsive tendencies [36]) (see S1 for details on the administered questionnaires). The research protocol consisted of two separate sessions: behavioral data were acquired during the first session, while the second was entirely devoted to resting state functional connectivity data acquisition. Both sessions began with a brief questionnaire to exclude the effects of potential confounding variables (e.g., smoke, caffeine consumption).

The behavioral session consisted of two computer-based tasks: a PCA and a Threshold Measurement Task. The PCA task was developed by Experiment Builder software (SR Research Ltd., version 2.4), while the Threshold Measurement Task was developed using the Matlab environment (Matlab R2021a). Both tasks were run on a Dell desktop computer with a 1920×1080 pixels screen at a viewing distance of 57 cm with the same visual background.

Pavlovian conditioning approach (PCA) task

The experimental session started with calibration of the eye-tracker device, during which each participant fixated on nine specific points on the computer screen. Participants were asked to keep their head on a chin rest and freely explore the entire screen during the task. They were informed that their final payment would correspond to the amount earned during the task, although this always equaled 20 Euros. Task instructions were displayed on the screen (detailed in S2).

The task consisted of 44 response-independent conditioning trials. In each trial, two 4×4 cm grey boxes were displayed on the left (the Sign box) and right (the Goal box) side of a black screen, positioned 15 degrees from a central white square fixation point. One of two possible visual cues (a vertically or horizontally oriented Gabor patch) appeared for 5 s within the Sign box, while the Goal box was filled with dynamic grey noise. One visual cue was associated with a reward for 20 trials (horizontal Gabor, CS+ trials), while the other cue was associated with no-reward for 24 trials (vertical Gabor, CS- trials). After the visual cue was removed, both the Sign and Goal boxes were empty for 500 ms, followed by the outcome (the presence or absence of the reward) presented for 1 s in the Goal box while the Sign box remained empty. The reward was represented by a coin picture displayed in the Goal box (different € values: 20 and 50 cents, 1 and 2 €, randomly presented for a total of 20 €); the absence of reward was represented by a scrambled coin picture in the Goal box (Fig. 1A). Reward presentation was accompanied with the sound of a falling coin. CS+ and CS- trials were randomized and presented with a variable inter-trial interval (ITI) (randomly alternating 1, 2, 3, or 4 s). After the first 10 trials (6

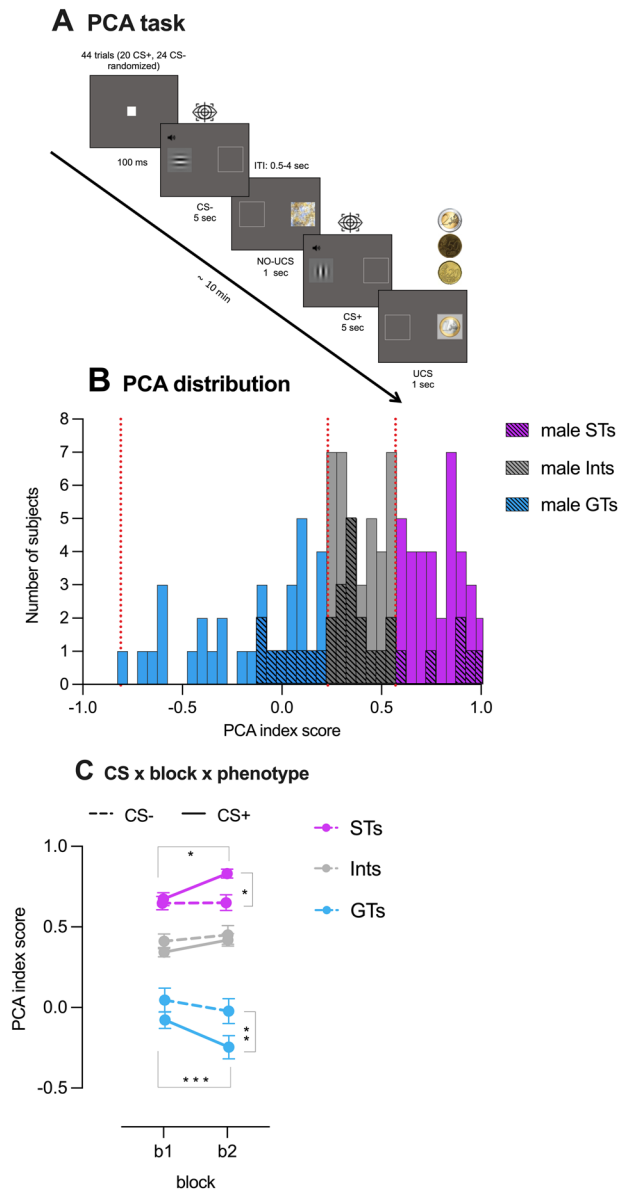


Fig. 1 Timeline of the PCA task. Timeline of the Pavlovian conditioning approach task (PCA) (A). Distribution of PCA scores for male (darker colors) and female (lighter colors) participants (B). PCA scores across the two blocks between the phenotypes (STs, GTs and Ints) for CS+ and CS- trials (C). Note. PCA Pavlovian conditioning approach, STs sign trackers, Ints intermediate trackers, GTs goal trackers. Red dotted lines in panel (B) indicate the phenotype split. Bars represent standard error of the mean. * $p < 0.05$; ** $p < 0.001$; *** $p < 0.0001$.

CS+ and 4 CS-), participants received the first earned amount of money to maintain the motivational value of the monetary reward, and then the task continued until the end. The entire task lasted approximately 10 min (see S3 for details).

Eye tracking

Eye movements were recorded in a dimly lit room only during the PCA task at 250 Hz using an infrared video-based eye tracker (Eyelink II plus; SR Research). Viewing was binocular, with the right eye being tracked. A chin rest was used to reduce head movements and maintain viewing distance. A 9-point calibration and validation were performed prior to the experiment.

Data acquired during the PCA task were analyzed offline using the EyeLink Data Viewer software package (SR Research Ltd., version 3.2). PCA

was based on different aspects of contiguous eye-gazes toward the cue and the reward location during CS presentation. Individual Dwell time (the total amount of time spent fixating the same box) during the 5 s of CS presentation was measured for two specific areas of interest: the Sign box and the Goal box.

Phenotypical categorization

Based on the index score used in rodent studies [1, 44], an eye-gaze PCA index – derived from the duration, number, and probability of fixations – was created. This index consists of the average of three difference scores for aspects of eye-gaze as follows: (1) dwell time [dwell time on Sign – dwell time on Goal/total dwell time], (2) frequency [trials with fixation on Sign – trials with fixation on Goal/total trials with fixations], and (3) probability [p of fixation on Sign – p of fixation on Goal/ p of Sign + p of Goal fixation] (p = trials with the event/total trials). A PCA score of +1 indicates that all responses were directed to the Sign box, a score of -1 indicates that all responses were directed to the Goal box, and a score of zero indicates that responses were directed equally to both places. PCA scores were separately calculated for all CS+ and CS- trials. Participants were categorized based on the sample distribution of PCA scores of the 20 CS+ trials.

Threshold measurement task

Contrast threshold for the stimuli used in the PCA task was measured right after the PCA task to ensure that the phenotypes did not differ in perceptual processing of the stimuli used in the PCA task (detailed in S4).

MRI acquisition and preprocessing

The collection of MR images was conducted using a high-performance 3 T scanner (Siemens MAGNETOM Prisma, Syngo version VE11E), equipped with a 32-channel head coil and with high power shim amplifiers (S5 for more details on the MRI acquisition).

Preprocessing of functional data was performed by the minimal preprocessing pipelines for the Human Connectome Project (HCP) [45] implemented in the open-source Quantitative Neuroimaging Environment & Toolbox (QuNex) software suite [46].

Specifically, preprocessing was conducted in the following way [47]: first, HCP PreFreeSurfer, FreeSurfer and PostFreeSurfer pipelines were successively conducted on the T1 images. This step included correcting the gradient distortion, aligning repeated runs, removing the skull from the image, removing readout distortion, performing bias field correction, registering the image to the standard Montreal Neurological Institute (MNI) space, and producing tissue maps and surface files for pia and white matter for each participant, followed by down-sampling and registering surface files. Once structural preprocessing was complete, the HCP pipelines fMRIVolume and fMRISurface were used on the functional and resting images. This process included removing spatial distortions, realigning volumes to compensate for participant motion, registering the fMRI data to the structural information, reducing the bias field, normalizing the 4D image to a global mean, masking the data, and transferring the time series from the volume into the CIFTI standard space.

Functional data were further preprocessed through QuNex's internal functions (i.e., *extract_nuisance*, *preprocess_bold*) to remove artifactual noises (movement, ventricle, white matter, respiratory and pulse signals) and their first derivatives by regressing them out from the BOLD signal. Then, fMRI data were down sampled into the whole-brain cortical and subcortical Tian-Schaefer atlas [48], obtaining 432 fMRI time series for each participant.

Statistical analyses

After the phenotypical categorization, differences between the three phenotypes in socio-demographic and dispositional characteristics (i.e., scores on self-reported questionnaires) were first analyzed using one-way Analysis of Variance (ANOVA) for continuous variables and chi-square (χ^2) tests for categorical variables.

To closely mirror the statistical approach usually taken in animal studies on this topic, PCA scores were then analyzed using a three-way repeated measure ANOVA, with Phenotype (ST, GT, Ints) as the between-subjects factor and Block (1 and 2) and CS type (CS- and CS+) as the within-subjects factors. Blocks of CS+ trials included 10 trials each, while blocks of CS- trials included 12 trials each (see S6 for details on the 2-blocks methodological choice).

Given that the measures consist of repeated observations, the role of learning in the relationship between CS type and Dwell Time was investigated using random effects mixed regression models (R package: stats). This analysis was performed on 4 (instead of 2) Blocks to reduce the unbalanced ratio of the randomly presented CS+ and CS− between Blocks. Our hypothesis was modeled in considering Dwell Time on the Goal and on the Sign boxes as the dependent variables, in two different models. Phenotype (ST, GT, Ints), Block (1, 2, 3, 4), CS type (CS− and CS+), and their interactions were included as fixed factors in both models; Participants and Trials as random factors. Mixed models are, however, characterized by difficulties in estimating degrees of freedom leading to potential unreliability of *p*-values. Therefore, the strength of the predictors within the models was further estimated by comparing the Akaike information criterion (AIC) and Bayesian information criterion (BIC) differences between models with and without the parameter of interest (Δ AIC and Δ BIC, respectively) [49]. Specifically, the parameter of interest was the 3-way Block \times Phenotype \times CS type interaction, which is the most relevant variable for our hypotheses. Denominator degrees of freedom were estimated by Satterthwaite and Kenward-Roger methods. Significant effects were further examined using Sidak's corrected post-hoc tests. In doing so, we focused on the theoretically relevant comparisons for the Block \times Phenotype \times CS type interaction, namely the difference between Block 1 and Block 4 in CS+ and CS− and differences between Phenotypes in Block 4 for CS+.

Brain topology and resting-state functional connectivity analyses

Whole-brain resting state functional connectivity was calculated by computing Pearson correlations between pairs of time series; these correlation values were then normalized with Fisher z-transformation and a 0.2 threshold was applied to the resulting correlation matrix. On the resultant 432 \times 432 symmetric signed network, eigenvector centrality [50] was computed on the nodes belonging to the cortico-striatal-thalamic network. Eigenvector centrality estimates and quantifies the influence of a node within the entire network; nodes having high eigenvector centrality are strongly connected to other important network nodes. Based on brain areas relevant for ST/GT phenotypical variation in rodent studies [42, 51, 52], 13 regions of interest (ROIs) were identified (see S7 for the full list). Subsequently, each pair of connections between the ROIs was extracted from the whole-brain connectivity matrix (left and right) resulting in a 26 \times 26 symmetric signed network.

To evaluate differences in resting state functional connectivity between STs and GTs, eigenvector centrality and brain connectivity data were subjected to a series of independent ANOVAs for each of the selected brain regions, covarying for biological sex. Significant group main effects for each variable of interest were followed by simple-effects analyses comparing STs and GTs.

At the post-hoc level, Sidak's corrected *p* are reported.

Given our aim to identify differences in resting state functional connectivity between STs and GTs, Ints were excluded from these analyses. However, analyses considering the dimensional value of PCA (along a continuum) were also performed for both eigenvector centrality and resting state functional connectivity patterns.

Bayesian statistical analyses were conducted to complement classical statistical analyses [53, 54]. The default Cauchy distribution (fixed effects $r = 0.5$) was used as prior distribution since this is the first study exploring brain topology and functional connectivity of ST/GT variation. The Bayes factor (BF10) quantifies the amount of evidence in favor of the alternative hypothesis with $1 > \text{BF10} > 3$ indicating anecdotal evidence; $3 < \text{BF10} < 10$ indicating substantial evidence; $10 < \text{BF10} < 30$ indicating strong evidence; $30 < \text{BF10} < 100$ indicating very strong evidence; and $\text{BF10} > 100$ indicating extreme evidence for the alternative hypothesis [54].

RESULTS

Pavlovian conditioned approach (PCA) task

Participants were categorized based on the sample distribution of PCA scores calculated from the 20 CS+ trials (Fig. 1B). Data from 4 participants were excluded from the analysis due to technical issues during the task, resulting in a final sample of 105 participants (73 females; 20 ± 3.11 years). The top and bottom tertiles of this distribution were categorized as STs ($n = 36$, PCA score between +0.57 and +1.00) and GTs ($n = 35$, PCA score between +0.23 and −0.81), respectively. Those in the middle tertile were categorized as Ints ($n = 34$, PCA score between +0.24 and +0.56).

Results of the ANOVA and chi-square (χ^2) tests on socio-demographic and dispositional variables are reported in Table 1. In terms of sex distribution, 30 out of 73 (41%) female participants were STs, and 23 (31.5%) were GTs, while 6 out of 32 (19%) male participants were STs and 12 (37.5%) were GTs (Fig. 1B). Significant group differences emerged for scores on the OCI-R and the anticipatory subscale of the TEPS. Pairwise comparisons showed that Ints had lower scores on the OCI-R than STs and GTs ($p < 0.05$), with no significant differences between STs and GTs. Additionally, STs and Ints had higher scores on the anticipatory subscale of the TEPS compared to GTs ($p < 0.01$), with no significant differences between STs and Ints.

To ensure that the eye-gaze was an acquired conditioned response, PCA scores were analyzed using a repeated measures ANOVA with Phenotype (ST, GT and Ints) as the between-subjects

Table 1. Sociodemographic and dispositional characteristics of Sign Trackers (STs), Goal Trackers (GTs), and Intermediates (Ints).

	STs ($n = 36$)	Ints ($n = 34$)	GTs ($n = 35$)	F/χ^2	<i>p</i>
Age, Years	21.13 (2.13)	21 (1.56)	21.34 (2.79)	0.14	0.87
Sex, <i>n</i>	30 F, 6 M	20 F, 14 M	23 F, 12 M	5.67	0.06
BMI, Kg/m ²	21.80 (4.31)	22.05 (3.13)	21.16 (2.64)	0.60	0.55
Education, Years	12.83 (2.75)	10.94 (4.78)	11.17 (4.68)	2.17	0.12
Smoking Status, <i>y/n</i>	19/17	16/17	17/18	0.17	0.92
Cigarettes per Day, <i>n</i>	1.56 (2.01)	1.67 (1.84)	1.91 (2.21)	0.29	0.75
Alcohol, units/week	2.72 (1.93)	2.27 (2.26)	2.66 (2.05)	0.47	0.63
OCI-R	32.5 (14.59)	21.50 (13.95)	29.31 (18.32)	4.48	0.01*
BIS-non planning	24.03 (4.37)	23.35 (4.67)	23.74 (4.39)	0.21	0.81
BIS-motor	19.33 (4.15)	19.18 (4.39)	20.23 (4.22)	0.62	0.54
BIS-cognitive	17.34 (3.59)	17.91 (3.99)	17.80 (4.18)	2.09	0.13
TEPS-anticipatory	4.43 (0.62)	4.62 (0.66)	4.15 (0.56)	6.33	0.003**
TEPS-consummatory	4.57 (0.70)	4.68 (0.68)	4.45 (0.83)	0.91	0.40
STAI (trait)	49.36 (10.04)	47.65 (10.28)	51.63 (11.78)	1.19	0.31

BMI body mass index, *Y* yes, *N* no, OCI-R obsessive compulsive inventory-revised, BIS Barratt impulsiveness scale 11, TEPS temporal experience of pleasure scale, STAI state trait anxiety inventory.

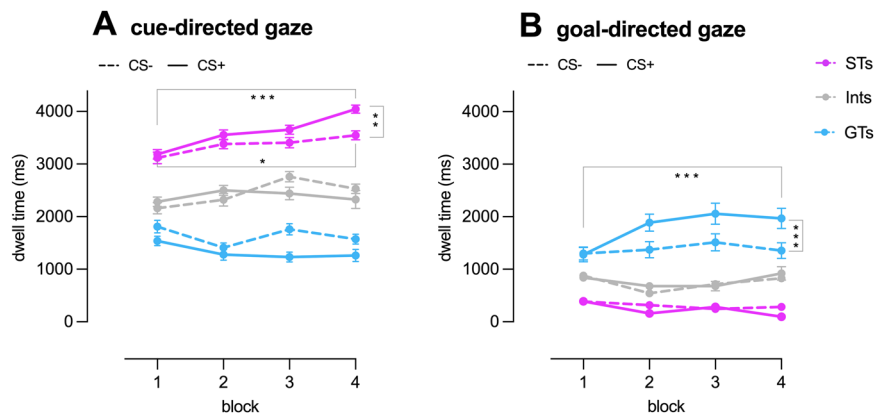


Fig. 2 Dwell Time Analysis. Dwell time on the Cue (panel **A**) and the Goal (panel **B**) for CS+ and CS– trials across the four blocks examined in the random effect regression models for the three phenotypes (STs, GTs, and Ints). Note. STs sign-trackers, Ints intermediates, GTs goal-trackers. Bars represent standard error of the mean. * $p < 0.05$; ** $p < 0.001$; *** $p < 0.0001$.

factor, and Block (1 and 2) and CS Type as within-subjects factors. Consistent with the phenotypization procedure, a main effect of Phenotype emerged [$F(2, 101) = 149.56, p < 0.001, \eta_p^2 = 0.79$], indicating that STs had higher PCA scores compared to Ints and GTs, and GTs had lower PCA scores compared to Ints and STs (all $ps < 0.0001$). The model also revealed the following significant interactions: (i) Phenotype \times Block [$F(2, 101) = 6.57, p = 0.002, \eta_p^2 = 0.12$], (ii) Phenotype \times CS Type [$F(2, 101) = 5.92, p = 0.004, \eta_p^2 = 0.11$], and (iii) Phenotype \times Block \times CS Type [$F(2, 101) = 6.83, p = 0.002, \eta_p^2 = 0.12$].

For the 3-way interaction, pairwise comparisons revealed no differences between CS+ and CS– trials during the first block. However, during the second block GTs had a greater tendency to direct the eye-gaze toward the Goal (as indicated by lower PCA score) during CS+ compared to CS– trials ($p < 0.001, d = 0.45$). STs showed higher PCA scores for CS+ compared to CS– in the second block, suggesting a greater tendency to direct the eye-gaze toward the Sign during CS+ trials than during CS– trials ($p = 0.03, d = 0.20$). Pairwise comparisons also revealed that PCA score changed from Block 1 to Block 2 for GTs ($p < 0.0001, d = 0.32$) and STs ($p = 0.002, d = 0.22$) for CS+ only, thus evidencing acquisition of the conditioned response. No differences emerged for Ints (Fig. 1C).

To assess learning of the conditioned responses to the CS+, the duration of eye gaze—a measure not directly used for phenotypical categorization—was examined using random effect mixed regression models. The first random effects regression model tested the main and interaction effects of CS type, Block, and Phenotype on Dwell Time on the sign. The model revealed significant main effects of Phenotype [$F(2, 103) = 75.05, p < 0.0001$] and Block [$F(3, 4502) = 7.79, p < 0.0001$]. Significant Phenotype \times Block [$F(6, 4502) = 10.30, p < 0.0001$] and Phenotype \times CS [$F(2, 4495) = 19.33, p < 0.0001$] interactions also emerged. A statistical trend that did not reach significance emerged for the Phenotype \times Block \times CS interaction [$F(6, 4565) = 1.93, p = 0.072$]. For the main effects, Dwell Time on the sign (in ms) was higher for i) STs (3461.06 (1329.44)) compared to GTs (1497.66 (1427.77)) and Ints (2445.07 (1462.17)) (all $ps < 0.001$); and ii) blocks 3 (2567.48 (1655.24)) and 4 (2561.93 (1691.49)) compared to block 1 (2355.18 (1509.41)); $p = 0.001$ and $p = 0.002$, respectively).

The difference in AIC and BIC between the model with the three-way interaction and the model without it was -75.9 for ΔAIC and -37.3 for ΔBIC , respectively, indicating that the model incorporating the three-way interaction better fit the data compared to the model without this parameter (see Table S8a).

The marginally significant three-way Phenotype \times CS \times Block interaction revealed that STs were characterized by higher Dwell Time on the Sign in Block 4 compared to Block 1 for both CS+

($p < 0.0001$) and CS– ($p = 0.002$), with significantly higher values in CS+ compared to CS– in Block 4 ($p = 0.0003$). No significant differences emerged for GTs and Ints in the examined theoretically relevant comparisons. At a between-level, Dwell Time on the Sign in Block 4 for CS+ was higher in STs compared to GTs ($p < 0.0001$) and Ints ($p = 0.0001$) and in Ints compared to GTs ($p = 0.002$) (Fig. 2A).

The second random effects regression model tested main effects and interactions of CS type, Block, and Phenotype on Dwell Time on the Goal. Phenotype [$F(2, 104) = 96.28, p < 0.0001$], Block [$F(3, 4507) = 4.06, p = 0.007$], and CS type [$F(1, 4496) = 27.70, p < 0.0001$] were significant predictors of Dwell Time on the Goal. Significant Phenotype \times Block [$F(6, 4507) = 12.18, p < 0.0001$], Phenotype \times CS [$F(2, 4496) = 36.59, p < 0.0001$], and Phenotype \times Block \times CS [$F(6, 4560) = 2.57, p = 0.017$] interactions emerged. As to main effects, Dwell Time on the Goal (in ms) was higher for (i) GTs (1560.46 (1402.55)) compared to STs (278.81 (642.92)) and Ints (758.64 (1017.38)), with significant differences between all three phenotypes (all $ps < 0.001$); (ii) block 4 (924.51 (1320.5)) compared to blocks 1 (821.17 (1204.07)); $p = 0.03$, 2 (844.17 (1177.02)); $p = 0.03$, and 3 (855.75 (1038.38)); $p = 0.01$; and (iii) CS+ (933.04 (1240.41)) compared to CS– (801.7 (1142.12)) ($p < 0.001$).

The difference between the model with and without the three way interaction was -76.9 for ΔAIC and -38.3 for ΔBIC , respectively. This suggests that the model incorporating CS, Block, Phenotype, and their two-way and three-way interactions as predictors best fit the data (see Table S8b).

The significant three-way interaction was further examined post-hoc. For GTs, a higher Dwell Time on the Goal was observed in Block 4 compared to Block 1 for CS+ ($p < 0.0001$) and for CS+ compared to CS– in Block 4 ($p < 0.0001$). STs showed the opposite pattern, with a lower Dwell Time on the Goal in Block 4 compared to Block 1 for CS+ ($p = 0.0004$) and for CS+ compared to CS– in Block 4 ($p = 0.04$). No significant differences in the examined theoretically relevant comparisons emerged for Ints. At a between-level, Dwell Time on the Goal in Block 4 for CS+ was higher in GTs compared to STs and Ints ($ps < 0.0001$) and in Ints compared to STs ($p = 0.003$) (Fig. 2B).

Brain topology and resting state functional connectivity

Analyses of brain topology revealed a significant main effect of Phenotype for the eigenvector centrality of right [$F(1, 23) = 9.73, p = 0.005, BF_{10} = 11.291$] and left putamen [$F(1, 23) = 7.35, p = 0.01, BF_{10} = 5.261$], right [$F(1, 23) = 3.81, p = 0.06, BF = 1.388$] and left insula [$F(1, 23) = 6.43, p = 0.02, BF = 3.244$] and right globus pallidus [$F(1, 23) = 7.97, p = 0.01, BF = 5.093$]. Simple-effects analyses indicated that those nodes were more central in STs compared to GTs (Fig. 3A and Table S9).

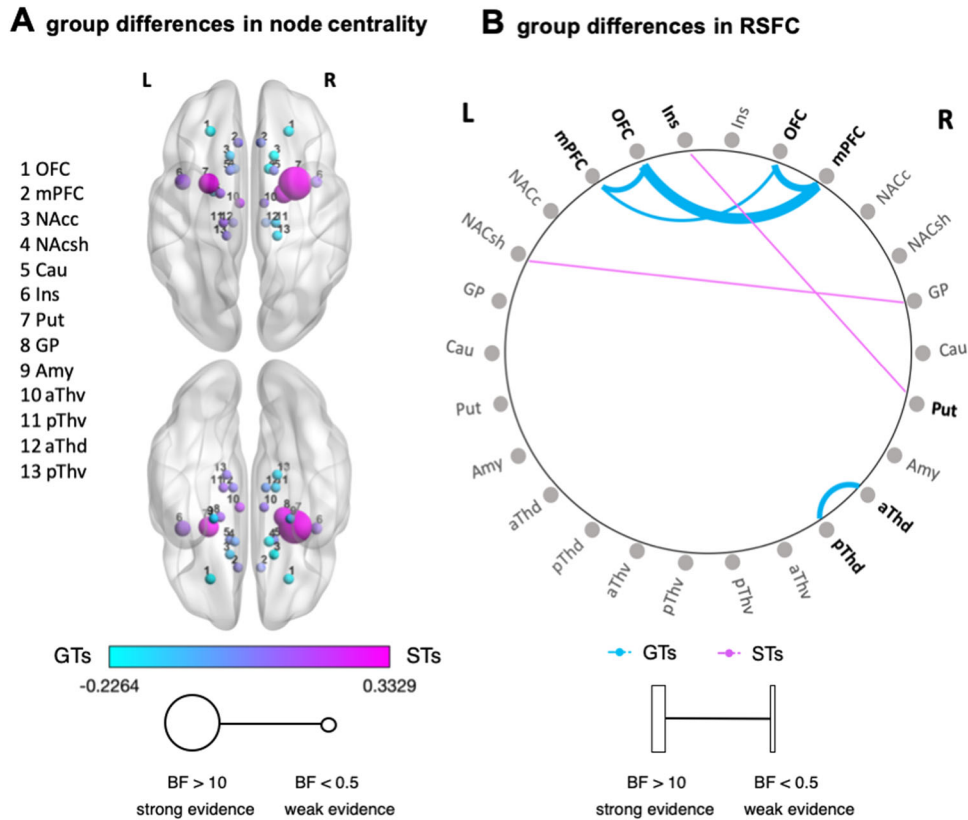


Fig. 3 Correlations between the PCA score and Eigenvector centrality. The node colors depict the normalized group mean of centrality (STs – GTs/STs + GTs) where more positive values corresponds to STs (pink) and more negative values to GTs (blue). The node size indicates the amount of Bayesian evidence for the alternative hypothesis where larger circles correspond to stronger Bayesian evidence for a significant mean difference of node centrality (A). Statistically significant group differences in resting state functional connectivity patterns. The strength of the connection indicates the amount of Bayesian evidence for the alternative hypothesis (B). Note. STs sign-trackers, GTs goal-trackers, OFC orbitofrontal cortex, mPFC medial prefrontal cortex, NAcc nucleus accumbens, NAcsh nucleus accumbens shell, Cau caudate, Ins insula, Put putamen, GP globus pallidus, Amy amygdala, aThv anterior ventral thalamus, pThv posterior ventral Thalamus, aThd Anterior dorsal Thalamus, pThd posterior dorsal thalamus.

When the phenotypical variance was considered along a continuum (including Ints), a significant positive correlation was found between PCA scores and the centrality of right globus pallidus ($r = 0.39$, $p = 0.03$). Conversely, a significant negative correlation emerged between PCA scores and the centrality of the right orbitofrontal cortex (OFC) ($r = -0.30$, $p = 0.04$).

Comparisons based on resting state functional connectivity revealed that STs had significantly lower connectivity between the right medial prefrontal cortex (mPFC) and left [F(1, 23) = 17.03, $p < 0.0001$, BF10 = 68.837] and right OFC [F(1, 23) = 11.43, $p = 0.003$, BF10 = 15.598], between the left mPFC and right [F(1, 23) = 6.35, $p = 0.02$, BF10 = 3.362] and left [F(1, 23) = 10.063, $p = 0.004$, BF10 = 10.545] OFC, and between the right dorsal anterior thalamus and right dorsal posterior thalamus [F(1, 23) = 9.452, $p = 0.005$, BF10 = 5.261] compared to GTs. Additionally, STs showed significantly higher resting state functional connectivity between the left insula and right putamen [F(1, 23) = 4.96035, $p = 0.04$, BF10 = 2.226] and between the right globus pallidus and the left NAc shell [F(1, 23) = 6.323, $p = 0.02$, BF10 = 3.066] compared to GTs (Fig. 3B and Table S10).

When phenotypical variance was considered along a continuum (including Ints), significant negative associations were observed between PCA scores and resting state functional connectivity between the right mPFC and the right ($r = 0.48$, $p < 0.0001$) and left OFC ($r = -0.47$, $p < 0.0001$).

DISCUSSION

In the present study, a PCA task was used to characterize the tendency to direct the eye-gaze toward the cue signaling the imminent reward delivery (Sign) or toward the location of reward delivery even if not yet available (Goal). A new fully appetitive Pavlovian task was developed to overcome the limitations of previous studies assessing ST/GT phenotypes by eye-tracking [37, 39]. Key improvements include: (i) using only rewarded trials for phenotypical categorization and ensuring that reward delivery was entirely response-independent; (ii) allowing voluntary eye-gaze direction toward one of the two boxes, with reward anticipation prevented by a variable interstimulus interval; and (iii) presenting a concrete reward image (€ coins) with an implicit contingency between the stimulus (CS) and the reward, similar to animal PCA paradigms.

Over the course of the task, participants categorized as GTs learned the contingency, exhibiting conditioned responses exclusively to CS+ trials. They progressively valued the reward delivery location and increasingly directed their eye-gaze toward the empty box. Participants categorized as STs did not exhibit the same distinct learning curve; instead, they demonstrated a pattern characterized by a general attraction to cues with potential predictive value, as evidenced by increased eye-gaze toward both the CS+ and the CS-. However, they ultimately placed greater value on the CS+ trials compared to the CS- trials. Crucially, previous studies conducted in humans have consistently reported a pattern of immediate attraction to predictive cues in STs that

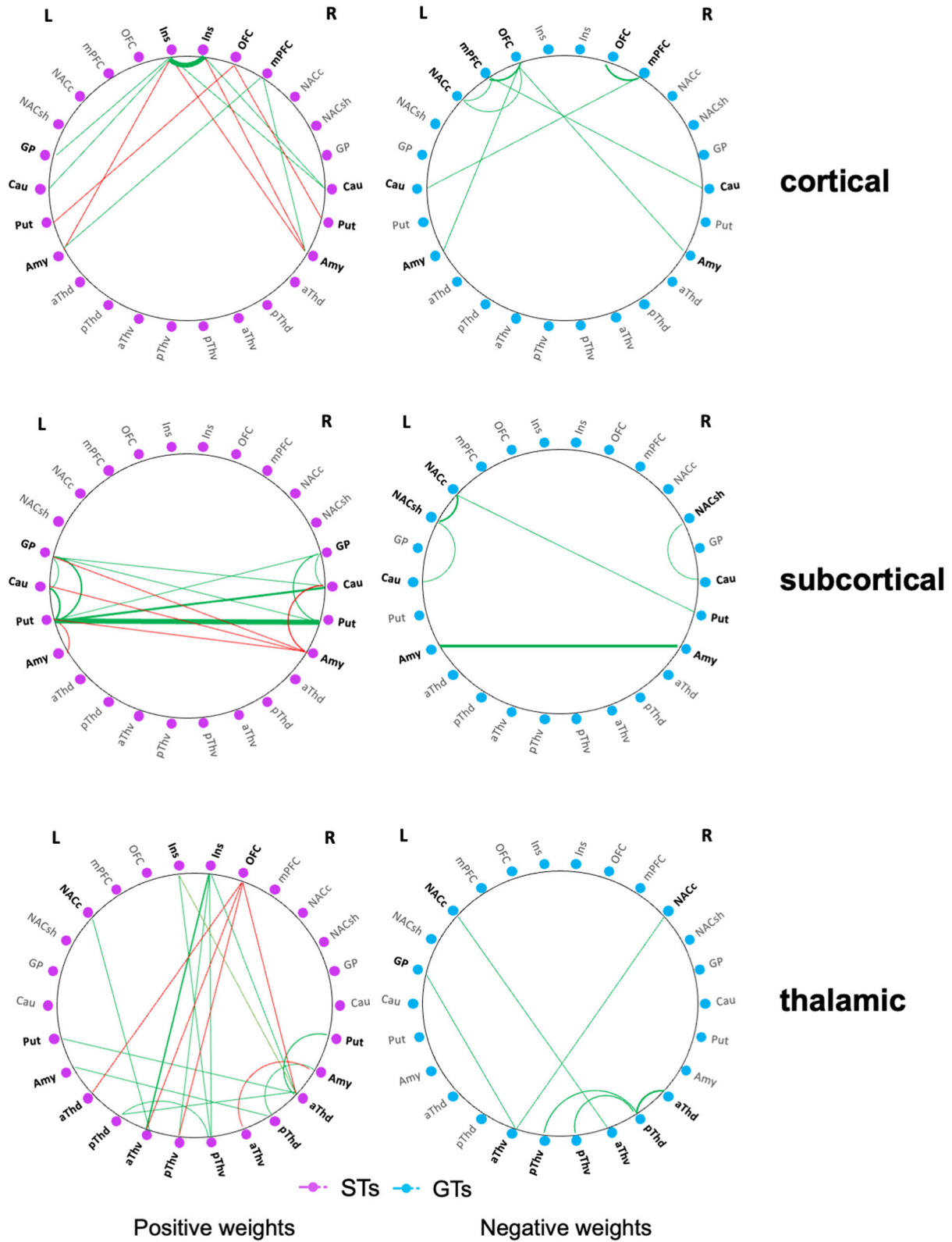


Fig. 4 Group specific resting state functional connectivity patterns in sign-trackers (STs) and goal-trackers (GTs) in the selected cortical, subcortical and thalamic regions. Note. The thickness of the lines reflects the strength of the correlation ($>$ thickness \Rightarrow Pearson's correlation coefficients). STs sign-trackers, GTs goal-trackers, OFC orbitofrontal cortex, mPFC medial prefrontal cortex, NACC nucleus accumbens, NACsh nucleus accumbens shell, Cau caudate, Ins insula, Put putamen, GP globus pallidus, Amy amygdala, aThv anterior ventral thalamus, pThv posterior ventral thalamus, aThd anterior dorsal thalamus, pThd posterior dorsal thalamus.

emerges early in tasks [40, 41, 55]. The only study that observed a clear learning pattern of the sign-tracking response over time used an extendable/retractable lever as the CS+ and measured attraction through physical contact with the lever [38]. This tendency of STs to attribute excessive motivational significance to predictive cues, regardless of their emotional valence, is well documented as a mechanism that increases the risk of developing psychopathological conditions, such as substance use disorder [56]. Importantly, behavioral differences between the groups were not attributable to differences in perceptual processing of the stimuli, as indicated by the threshold assessment task results.

To our knowledge, this is the first study to map sign-tracking and goal-tracking onto resting state functional connectivity patterns. Although preliminary, present findings support the hypothesis that the brain mechanisms identified in rats may also be relevant to human ST and GT endophenotypes.

Eigenvector centrality, a measure of functional connectivity, captures the influence that one node holds over information flow between all other relevant nodes in the network [57]. At the group level, STs exhibited higher centrality in the bilateral putamen, bilateral insula, and right globus pallidus, reflecting the dominance of these structures—primarily part of the Salience Network [58]—in transferring information across the network in this phenotype. When we looked at the same data along a continuum, a higher tendency toward goal-tracking was associated with stronger centrality in the right OFC, indicating greater involvement of this structure in efficient pathways. These patterns mimic findings in animals, where sign tracking behavior is dominated by subcortical motivational systems and goal tracking behavior by more cortical processes [9, 28].

Resting state functional connectivity analyses further supported these centrality findings, showing increased connectivity between subcortical regions (left insula and right putamen; right globus pallidus and left NAc shell) and reduced connectivity between cortical regions (right mPFC and left OFC; left mPFC and bilateral OFC; right anterior dorsal thalamus and right posterior dorsal thalamus) in STs. Notably, stronger resting state functional connectivity between the right mPFC and bilateral OFC was associated with a higher tendency toward goal-tracking, examined along a continuum from sign- to goal-tracking. These results align with findings that GT rats exhibit efficient top-down control in attributing incentive salience to reward-paired cues compared to ST rats [10, 28].

Rodent studies also show that some brain areas are involved in both sign-tracking and goal-tracking phenotypes through different circuits balanced within the PVT, affecting NAc modulation [10]. Specifically, orexinergic innervation from the Lateral Hypothalamus to the PVT encodes the incentive motivational value of reward cues in ST rats [59, 60], while the glutamatergic innervation from the Prelimbic cortex to the PVT is likely responsible for this in GT rats [9]. This may explain the lack of between-group differences in NAc centrality in the present study, as this brain region may be a crucial hub in both STs and GTs.

The PVT, a small nucleus of the medial-dorsal midline thalamus, challenges the traditional view of thalamic nuclei as sensory relays, with the capacity to alter the state of downstream brain areas involved in motivated behaviors [61]. Recent high-resolution resting-state MRI investigations support the extensive functional connectivity of the PVT [62]. We selected the dorsal and ventral thalamus as the closest anatomical divisions to represent the PVT. The lack of between-group differences in the centrality of thalamic nodes suggests that they may play crucial roles in both phenotypes. However, current data indicates higher resting state functional connectivity between the anterior and posterior divisions of the dorsal thalamus in GTs compared to STs (Figs. 3B, 4) and phenotype-dependent connectivity differences of thalamic nodes within the cortico-striatal-thalamic circuit (Fig. 4). These findings support the role of thalamic nuclei, particularly the

PVT, as functional gates to subcircuits involved in motivated behaviors [61]. A previous task-related fMRI study found evidence of brain lateralization effects when examining neural correlates of these phenotypes [40], with current results indicating a right-hemisphere dominance in STs. However, limited data precludes firm conclusions on this issue.

Despite methodological rigor, the present study has some limitations. The sample was predominantly female, with most women categorized as STs (Fig. 1B and Table 1). This is consistent with findings that females are generally more cue-dependent (e.g., [63]) and with a recent study reporting a skewed distribution of female participants toward sign-tracking [38]. However, preclinical literature presents contradictory evidences on sex-differences, with female rats being more STs [64–67], equally STs as male rats [68–71], or showing faster acquisition of sign-tracking when young [68], or after early alcohol exposure [72, 73]. The young age of the present sample may influence the reported sex differences in ST/GT phenotypic variation. Additionally, due to exclusion criteria for the functional resonance imaging session, such data was collected from a subsample of participants, leading to an unequal distribution of STs and GTs in the functional imaging analysis. To mitigate bias, we conducted both group and dimensional analyses, obtaining consistent findings. Despite selecting a limited number of regions based on empirical findings from the preclinical literature and correcting for multiple comparisons, a high number of univariate tests were conducted on data deriving from a relatively small sample. Identifying small brain structures precisely is challenging, which may explain the lack of observed NAc role in centrality analyses. Contrary to previous reports [22–24], no differences emerged in self-reported traits such as impulsivity or obsessive-compulsive tendencies, likely due to our sample's good mental health. Other studies also failed to find associations between sign-tracking and impulsivity [40, 41]. However, compared to GTs, STs and Ints scored higher on the anticipatory (but not consummatory) pleasure scale, aligning with their enhanced attraction to reward-related cues.

While our measures do not quantify the directional causality of brain region interactions, this study preliminarily supports the translational validity of the ST/GT phenotyping in humans. Greater susceptibility to reward-related cue attraction (as in STs) may increase vulnerability to dysfunctional or risky behaviors, such as drug use or compulsivity. Translating the ST/GT paradigm to humans could enable early identification of such vulnerability patterns, ultimately aiding in the development of precision-psychiatry-based prevention and intervention programs.

DATA AVAILABILITY

The deidentified dataset is available on request to researchers who meet the criteria for confidential information, by sending a request to the corresponding author.

REFERENCES

- Robinson TE, Flagel SB. Dissociating the predictive and incentive motivational properties of reward-related cues through the study of individual differences. *Biol Psychiatry*. 2009;65:869–73. <https://doi.org/10.1016/j.biopsych.2008.09.006>.
- Robinson TE, Yager LM, Cogan ES, Saunders BT. On the motivational properties of reward cues: individual differences. *Neuropharmacol*. 2014;76:450–9. <https://doi.org/10.1016/j.neuropharm.2013.05.040>
- Flagel SB, Clark JJ, Robinson TE, Mayo L, Czuj A, Willuhn I, et al. A selective role for dopamine in stimulus-reward learning. *Nature*. 2011;469:53–7.
- Lesaint F, Sigaud O, Flagel SB, Robinson TE, Khamassi M. Modelling individual differences in the form of Pavlovian conditioned approach responses: a dual learning systems approach with factored representations. *PLoS Comput Biol*. 2015;10:e1003466. <https://doi.org/10.1371/journal.pcbi.1003466>
- Clark JJ, Hollon NG, Phillips PEM. Pavlovian valuation systems in learning and decision making. *Curr Op Neurobiol*. 2012. <https://doi.org/10.1016/j.conb.2012.06.004>.

6. Saunders BT, Robinson TE. The role of dopamine in the accumbens core in the expression of Pavlovian-conditioned responses. *Eur J Neurosci*. 2012;36:2521–32. <https://doi.org/10.1111/j.1460-9568.2012.08217.x>
7. Iglesias AG, Chiu AS, Wong J, Campus P, Li F, Liu Z, et al. Inhibition of dopamine neurons prevents incentive value encoding of a reward cue: with revelations from deep phenotyping. *J Neurosci*. 2023;43:7376–92. <https://doi.org/10.1523/JNEUROSCI.0848-23.2023>
8. Berridge KC. Parsing reward. *Trends Neurosci*. 2003;26:507–13. [https://doi.org/10.1016/S0166-2236\(03\)00233-9](https://doi.org/10.1016/S0166-2236(03)00233-9)
9. Campus P, Covelo IR, Kim Y, Parsegian A, Kuhn BN, Lopez SA, et al. The paraventricular thalamus is a critical mediator of top-down control of cue-motivated behavior in rats. *Elife*. 2019;8:e49041. <https://doi.org/10.7554/eLife.49041>
10. Iglesias AG, Flagel SB. The paraventricular thalamus as a critical node of motivated behavior via the hypothalamic-thalamic-striatal circuit. *Front Integr Neurosci*. 2021;15:706713. <https://doi.org/10.3389/fnint.2021.706713>
11. Saunders BT, Robinson TE. Individual variation in resisting temptation: implication for addiction. *Neurosci Biobehav Rev*. 2013;37:1955–75. <https://doi.org/10.1016/j.neubiorev.2013.02.008>
12. Belin D, Belin-Rauscent A, Everitt BJ, Dalley JW. In search of predictive endo-phenotypes in addiction: insights from preclinical research. *Genes Brain Behav*. 2016;15:74–88. <https://doi.org/10.1111/gbb.12265>
13. Robinson TE, Carr C, Kawa AB. The propensity to attribute incentive salience to drug cues and poor cognitive control combine to render sign-trackers susceptible to addiction. In *Sign-tracking and drug addiction* (eds Tomie A, Morrow, J) Ch. 4 (Ann Arbor, MI: Michigan Publishing, 2018). <https://doi.org/10.3998/mpub.10215070>
14. O'Brien CP, Childress AR, McLellan A, Ehrman R. A learning model of addiction. *Res Publ Assoc Res Nerv Ment Dis*. 1992;70:157–77.
15. Carter BL, Tiffany ST. Meta-analysis of cue-reactivity in addiction research. *Addiction*. 1999;94:327–40.
16. Meyer PJ, Ma ST, Robinson TE. A cocaine cue is more preferred and evokes more frequency-modulated 50-kHz ultrasonic vocalizations in rats prone to attribute incentive salience to a food cue. *Psychopharmacol*. 2012;219:999–1009. <https://doi.org/10.1007/s00213-011-2429-7>
17. Saunders BT, Robinson TE. A cocaine cue acts as an incentive stimulus in some but not others: implications for addiction. *Biol Psychiatry*. 2010;67:730–6. <https://doi.org/10.1016/j.biopsych.2009.11.015>
18. Yager LM, Robinson TE. A classically conditioned cocaine cue acquires greater control over motivated behavior in rats prone to attribute incentive salience to a food cue. *Psychopharmacol*. 2013;226:217–28. <https://doi.org/10.1007/s00213-012-2890-y>
19. Beckmann JS, Marusich JA, Gipson CD, Bardo MT. Novelty seeking, incentive salience and acquisition of cocaine self-administration in the rat. *Behav Brain Res*. 2011;216:159–65. <https://doi.org/10.1016/j.bbr.2010.07.022>
20. Tunstall BJ, Kearns DN. Sign-tracking predicts increased choice of cocaine over food in rats. *Behav Brain Res*. 2015;281:222–8. <https://doi.org/10.1016/j.bbr.2014.12.034>
21. Saunders BT, Robinson TE. Individual variation in the motivational properties of cocaine. *Neuropsychopharmacol*. 2011;36:1668–76. <https://doi.org/10.1038/npp.2011.48>
22. Tomie A, Grimes KL, Pohorecky LA. Behavioral characteristics and neurobiological substrates shared by Pavlovian sign-tracking and drug abuse. *Brain Res Rev*. 2008;58:121–35. <https://doi.org/10.1016/j.brainresrev.2007.12.003>
23. Lovic V, Saunders BT, Yager LM, Robinson TE. Rats prone to attribute incentive salience to reward cues are also prone to impulsive action. *Behav Brain Res*. 2011;223:255–61. <https://doi.org/10.1016/j.bbr.2011.04.006>
24. King CP, Palmer AA, Woods Solberg, Hawk LC, Richards LA, Meyer JB. PJ. Premature responding is associated with approach to a food cue in male and female heterogeneous stock rats. *Psychopharmacol*. 2016;233:2593–605. <https://doi.org/10.1007/s00213-016-4306-x>
25. Swann AC, Bjork JM, Moeller FG, Dougherty DM. Two models of impulsivity: relationship to personality traits and psychopathology. *Biol Psychiatry*. 2002;51:988–94. [https://doi.org/10.1016/S0006-3223\(01\)01357-9](https://doi.org/10.1016/S0006-3223(01)01357-9)
26. Kreek M, Nielsen D, Butelman E, Laforge K. Genetic influences on impulsivity, risk taking, stress responsivity and vulnerability to drug abuse and addiction. *Nat Neurosci*. 2005;8:1450–57. <https://doi.org/10.1038/nn1583>
27. Verdejo-García A, Lawrence AJ, Clark L. Impulsivity as a vulnerability marker for substance-use disorders: review of findings from high-risk research, problem gamblers and genetic association studies. *Neurosci Biobehav Rev*. 2008;32:777–810. <https://doi.org/10.1016/j.neubiorev.2007.11.003>
28. Sarter M, Phillips KB. The neuroscience of cognitive-motivational styles: sign-and goal-trackers as animal models. *Behav Neurosci*. 2018;132:1–12. <https://doi.org/10.1037/bne0000226>
29. Anselme P, Robinson MJF. From sign-tracking to attentional bias: implications for gambling and substance use disorders. *Prog Neuropharmacol Biol Psychiatry*. 2020;99:109861 <https://doi.org/10.1016/j.pnpb.2020.109861>
30. Field M, Cox WM. Attentional bias in addictive behaviors: a review of its development, causes, and consequences. *Drug Alcohol Depend*. 2008;97:1–20. <https://doi.org/10.1016/j.drugalcdep.2008.03.030>
31. Zhang M, Ying J, Wing T, Song G, Fung D, Smith H. A systematic review of attention biases in opioid, cannabis, stimulant use disorders. *Int J Environ Res Public Health*. 2018;15:1138 <https://doi.org/10.3390/ijerph15061138>
32. Van Gucht D, Vansteenwegen D, Van den Bergh O, Beckers T. Conditioned craving cues elicit an automatic approach tendency. *Behav Res Ther*. 2008;46:1160–69. <https://doi.org/10.1016/j.brat.2008.05.010>
33. Le Pelley ME, Pearson D, Griffiths O, Beesley T. When goals conflict with values: counterproductive attentional and oculomotor capture by reward-related stimuli. *J Exp Psychol: General*. 2015;144:158–71. <https://doi.org/10.1037/xge0000037>
34. Anderson BA, Faulkner ML, Rilee JJ, Yantis S, Marvel CL. Attentional bias for nondrug reward is magnified in addiction. *Exp Clinical Psychopharmacol*. 2013;21:499–506. <https://doi.org/10.1037/a0034575>
35. Albertella L, Jvd Hooven, Bovens R, Wiers RW. Reward-related attentional capture predicts non-abstinence during a one-month abstinence challenge. *Addictive Behav*. 2021;114:106745. <https://doi.org/10.1016/j.addbeh.2020.106745>
36. Schettino M, Ceccarelli I, Tarvainen M, Martelli M, Orsini C, Ottaviani C. From skinner box to daily life: sign-tracker phenotype co-segregates with impulsivity, compulsivity, and addiction tendencies in humans. *Cogn Affect Behav Neurosci*. 2022;22:1358–69. <https://doi.org/10.3758/s13415-022-01014-y>
37. Garofalo S, Di Pellegrino G. Individual differences in the influence of task-irrelevant Pavlovian cues on human behavior. *Front Behav Neurosci*. 2015;9:63 <https://doi.org/10.3389/fnbeh.2015.00163>
38. Cope LM, Gheidi A, Martz ME, Duval ER, Khalil H, Allerton T, et al. A mechanical task for measuring sign- and goal-tracking in humans: a proof-of-concept study. *Behav Brain Res*. 2023;436:114112. <https://doi.org/10.1016/j.bbr.2022.114112>
39. Schad DJ, Rapp MA, Garbusow M, Nebe S, Sebold M, Obst E, et al. Dissociating neural learning signals in human sign- and goal-trackers. *Nat Hum Behav*. 2020;4:201–14. <https://doi.org/10.1038/s41562-019-0765-5>
40. Colaizzi JM, Flagel SB, Gearhardt AN, Borowitz MA, Kupicki R, Zotev V, et al. The propensity to sign-track is associated with externalizing behavior and distinct patterns of reward-related brain activation in youth. *Sci Rep*. 2023;13:4402 <https://doi.org/10.1038/s41598-023-30906-3>
41. Dinu LM, Georgescu AL, Singh SN, Byrom NC, Overton PG, Singer BF, et al. Sign-tracking and goal-tracking in humans: utilising eye-tracking in clinical and non-clinical populations. *Behav Brain Res*. 2024;461:114846 <https://doi.org/10.1016/j.bbr.2024.114846>
42. Flagel SB, Robinson TE. Neurobiological basis of individual variation in stimulus-reward learning. *Curr Opin Behav Sci*. 2017;13:178–85. <https://doi.org/10.1016/j.cobeha.2016.12.004>
43. Deisseroth K. Circuit dynamics of adaptive and maladaptive behaviour. *Nature*. 2014;505:309–17. <https://doi.org/10.1038/nature12982>
44. Campus P, Accoto A, Maiolati M, Latagliata C, Orsini C. Role of prefrontal 5-HT in the strain-dependent variation in sign-tracking behavior of C57BL/6 and DBA/2 mice. *Psychopharmacol*. 2016;233:1157–69. <https://doi.org/10.1007/s00213-015-4192-7>
45. Glasser MF, Sotiropoulos SN, Wilson JA, Coalson TS, Fischl B, Andersson JL, et al. The minimal preprocessing pipelines for the Human Connectome Project. *NeuroImage*. 2013;80:105–24. <https://doi.org/10.1016/j.neuroimage.2013.04.127>
46. Ji JL, Spronk M, Kulkarni K, Repovš G, Anticevic A, Cole MW. Mapping the human brain's cortical-subcortical functional network organization. *NeuroImage*. 2019;185:35–57. <https://doi.org/10.1016/j.neuroimage.2018.10.006>
47. Wang S, Zhang Y, Zhang X, Sun J, Lin N, Zhang J, et al. An fMRI dataset for concept representation with semantic feature annotations. *Sci Data*. 2022;9:721.
48. Tian Y, Margulies DS, Breakspear M, Zalesky A. Topographic organization of the human subcortex unveiled with functional connectivity gradients. *Nat Neurosci*. 2020;1421–32. <https://doi.org/10.1038/s41593-020-00711-6>
49. Wagenmakers EJ, Farrell S. AIC model selection using Akaike weights. *Psychon Bull Rev*. 2004;11:192–6. <https://doi.org/10.3758/bf03206482>
50. Rubinov M, Sporns O. Weight-conserving characterization of complex functional brain networks. *NeuroImage*. 2011;56:2068–79. <https://doi.org/10.1016/j.neuroimage.2011.03.069>
51. Flagel SB, Cameron CM, Pickup KN, Watson SJ, Akil H, Robinson TE. A Food predictive cue must be attributed with incentive salience for it to induce c-Fos mRNA expression in cortico-striatal-thalamic brain regions. *Neurosci*. 2011;196:80–96. <https://doi.org/10.1016/j.neuroscience.2011.09.004>
52. Yager LM, Pitchers KK, Flagel SB, Robinson TE. Individual variation in the motivational and neurobiological effects of an opioid cue. *Neuropsychopharmacol*. 2015;40:1269–77. <https://doi.org/10.1038/npp.2014.314>
53. Keyzers C, Gazzola V, Wagenmakers EJ. Using Bayes factor hypothesis testing in neuroscience to establish evidence of absence. *Nat Neurosci*. 2020;23:788–99. <https://doi.org/10.1038/s41593-020-0660-4>
54. Jeffreys, H. *Theory of Probability*. OUP Oxford 1998.

55. Cherkasova MV, Clark L, Barton JJS, Stoessl AJ, Winstanley CA. Risk-promoting effects of reward-paired cues in human sign- and goal-trackers. *Behav Brain Res.* 2024;461:114865 <https://doi.org/10.1016/j.bbr.2024.114865>
56. Morrow JD, Saunders BT, Maren S, Robinson TE. Sign-tracking to an appetitive cue predicts incubation of conditioned fear in rats. *Behav Brain Res.* 2015;276:59–66. <https://doi.org/10.1016/j.bbr.2014.04.002>
57. Bullmore E, Sporns O. Complex brain networks: graph theoretical analysis of structural and functional systems. *Nat Rev Neurosci.* 2009;10:186–98. <https://doi.org/10.1038/nrn2575>
58. Seeley WW. The salience network: a neural system for perceiving and responding to homeostatic demands. *J Neurosci.* 2019;39:9878–82. <https://doi.org/10.1523/JNEUROSCI.1138-17.2019>
59. Haight JL, Fuller ZL, Fraser KM, Flagel SB. A food-predictive cue attributed with incentive salience engages subcortical afferents and efferents of the paraventricular nucleus of the thalamus. *Neurosci.* 2017;340:135–52. <https://doi.org/10.1016/j.neuroscience.2016.10.043>
60. Haight JL, Campus P, Maria-Rios CE, Allison JM, Klumpner MS, Kuhn BN, et al. The lateral hypothalamus and orexinergic transmission in the paraventricular thalamus promote the attribution of incentive salience to reward-associates cues. *Psychopharmacol.* 2020;237:3741–58. <https://doi.org/10.1007/s00213-020-05651-4>
61. McGinty JF, Otis JM. Heterogeneity in the paraventricular thalamus: the traffic light of motivated behaviors. *Front Behav Neurosci.* 2020;14:590528 <https://doi.org/10.1007/s00213-020-05651-4>
62. Kark SM, Birnie MT, Baram TZ, Yassa MA. Functional connectivity of the human paraventricular thalamic nucleus: insights from high field functional MRI. *Front Integr Neurosci.* 2021;15:662293 <https://doi.org/10.3389/fnint.2021.662293>
63. Stoet G. Sex differences in the Simon task help to interpret sex differences in selective attention. *Psychol Res.* 2017;81:571–81. <https://doi.org/10.1007/s00426-016-0763-4>
64. Peterson VL, Richards JB, Meyer PJ, Cabrera-Rubio R, Tripi JA, King CP, et al. Sex-dependent associations between addiction-related behaviors and the microbiome in outbred rats. *EBioMedicine.* 2020;55:1027669. <https://doi.org/10.1016/j.ebiom.2020.102769>
65. Stringfield SJ, Madayag AC, Boettiger CA, Robinson DL. Sex differences in nicotine-enhanced Pavlovian conditioned approach in rats. *Biol Sex Differ.* 2019;10:37 <https://doi.org/10.1186/s13293-019-0244-8>
66. Hughson AR, Hovarth AP, Holl K, Palmer AA, Solberg Woods LA, Robinson TE, et al. Incentive salience attribution, “sensation-seeking” and “novelty-seeking” are independent traits in a large sample of male and female heterogeneous stock rats. *Sci Rep.* 2019;9:2351 <https://doi.org/10.1038/s41598-019-39519-1>
67. King CP, Tripi JA, Hughson AR, Horvath AP, Lamparelli AC, Holl KL, et al. Sensitivity to food and cocaine cues are independent traits in a large sample of heterogeneous stock rats. *Sci Rep.* 2021;11:2223. <https://doi.org/10.1038/s41598-020-80798-w>
68. Hammerslag LR, Gullely JM. Age and sex differences in reward behavior in adolescent and adult rats. *Dev Psychobiol.* 2014;56:611–21. <https://doi.org/10.1002/dev.21127>
69. Pitchers KK, Flagel SB, O'Donnell EG, Woods LC, Sarter M, Robinson TE. Individual variation in the propensity to attribute incentive salience to a food cue: influence of sex. *Behav Brain Res.* 2015;278:462–9. <https://doi.org/10.1016/j.bbr.2014.10.036>
70. Zumbusch A, Samson A, Chernoff C, Coslovich B, Hynes T. Biological sex influences the contribution of sign-tracking and anxiety-like behavior toward remifentanyl self-administration. *Behav Neurosci.* 2023;137:196–210. <https://doi.org/10.1037/bne0000551>
71. Bien E, Smith K. The role of sex on sign-tracking acquisition and outcome devaluation sensitivity in Long Evans rats. *Behav Brain Res.* 2023;455:114656 <https://doi.org/10.1016/j.bbr.2023.114656>
72. Madayag AC, Stringfield SJ, Reissner KJ, Boettiger CA, Robinson DL. Sex and adolescent ethanol exposure influence the pavlovian conditioned approach. *Alcohol Clin Exp Res.* 2017;41:846–56. <https://doi.org/10.1111/acer.13354>
73. Pickens CL, Cook A, Gaedert B. Dose-dependent effects of alcohol injections on omission-contingency learning have an inverted-U pattern. *Behav Brain Res.* 2020;392:112736 <https://doi.org/10.1016/j.bbr.2020.112736>

ACKNOWLEDGEMENTS

This work was supported by Sapienza Progetti di Ricerca Medi (RM12117A8A578DB4). The authors are grateful to Tania Moretta for her valuable contribution to the statistical data analysis. They authors also would like to thank Valeria Gigli, Federica Giudetti and Rachele Grimaldi for their help with the recruitment and behavioral data collection.

AUTHOR CONTRIBUTIONS

Study concept and design: MS, MMau, COT, MMar, and COR. Analysis and interpretation of results: MS, MMau, CP, IC, FG, AN, COT, MMar, and COR. Draft manuscript preparation: MS, MMau, IC, COT, and COR. Critical revision of the manuscript: MS, MMau, CP, IC, FG, AN, COT, MMar, and COR. All authors reviewed the results and approved the final version of the manuscript.

COMPETING INTERESTS

The authors declare no competing interests.

ETHICS APPROVAL AND CONSENT TO PARTICIPATE

The study was approved by the Institutional Review Board of the Department of Psychology (Prot. N. 547/2021) and by the Research Ethical Committee of IRCSS Santa Lucia Foundation (CE/PROG. 896). Informed consent was obtained from each participant.

ADDITIONAL INFORMATION

Supplementary information The online version contains supplementary material available at <https://doi.org/10.1038/s41398-024-03162-w>.

Correspondence and requests for materials should be addressed to Cristina Orsini.

Reprints and permission information is available at <http://www.nature.com/reprints>

Publisher's note Springer Nature remains neutral with regard to jurisdictional claims in published maps and institutional affiliations.



Open Access This article is licensed under a Creative Commons Attribution-NonCommercial-NoDerivatives 4.0 International License, which permits any non-commercial use, sharing, distribution and reproduction in any medium or format, as long as you give appropriate credit to the original author(s) and the source, provide a link to the Creative Commons licence, and indicate if you modified the licensed material. You do not have permission under this licence to share adapted material derived from this article or parts of it. The images or other third party material in this article are included in the article's Creative Commons licence, unless indicated otherwise in a credit line to the material. If material is not included in the article's Creative Commons licence and your intended use is not permitted by statutory regulation or exceeds the permitted use, you will need to obtain permission directly from the copyright holder. To view a copy of this licence, visit <http://creativecommons.org/licenses/by-nc-nd/4.0/>.

© The Author(s) 2024